Bulky substituent effects on the iron(III) complexation of 1,4,7-triazacyclononane

Jonathan L. Sessler*, John W. Sibert and Vincent Lynch
Department of Chemistry and Biochemistry, University of Texas at Austin, Austin, TX 78712 (USA)

(Received August 27, 1993)

Abstract

The synthesis of two sterically encumbered macrocycles, *N,N′,N″*-triisopropyl-1,4,7-triazacyclononane (**1**) and *N,N′,N″*-triisobutyl-1,4,7-triazacyclononane (**2**), and their reactions with iron(III) have been investigated. In alcoholic solvents, a 1.1 mixture of either **1** or **2** and $FeCl_3 \cdot 6H_2O$ does not result in complex formation. Instead, the macrocycles are singly protonated with the iron being incorporated into the anion. The structure of $(\mathbf{1} \cdot H)^+(FeCl_4)^-$ was determined by single crystal X-ray methods. Crystals are orthorhombic, space group *Pbca* (No. 61), with the following unit cell parameters: $a = 14.921(2)$, $b = 17.765(2)$, $c = 17.414(2)$ Å, $V = 4616.0(10)$ Å^3 and $Z = 8$. The structure of $(\mathbf{2} \cdot H)^+{}_2(Fe_2OCl_6)^{2-}$ was also determined. Crystals are triclinic, space group $P\bar{1}$ (No. 2) with the following unit cell parameters: $a = 9.3543(10)$, $b = 10\,1002(11)$, $c = 14.4167(14)$ Å, $\alpha = 85.185(8)$, $\beta = 73\,395(8)$, $\gamma = 73.198(8)°$, $V = 1246\,6(2)$ Å^3 and $Z = 2$. The reactivity of **1** and **2** with iron(III) is then compared to that of the well-studied macrocycles, 1,4,7-triazacyclononane and *N,N′,N″*-trimethyl-1,4,7-triazacyclononane. The inability of **1** and **2** to serve as ligands to iron(III) in protic media is attributed to steric interactions involving the bulky alkyl appendages of the macrocycles.

Key words: Crystal structures; Iron complexes; Macrocyclic ligand complexes

Introduction

The synthesis and metal-binding properties of saturated azamacrocycles have been extensively studied in recent years [1]. In particular, 1,4,7-triazacyclononane (TACN) and its *N,N′,N″*-trimethyl derivative [2] are known to coordinate a variety of transition metals and have been used to stabilize a μ-oxobis (μ-carboxylato)diiron core in hemerythrin-directed model studies [3]. In addition, a variety of TACN derivatives bearing from one to three pendant ligating groups have been investigated for their ability to further enhance metal coordination [4]. There has, however, been little attention directed toward the study of saturated azamacrocycles which contain bulky, non-coordinating substituents and their effects on the coordination chemistry of the macrocycle [5]. These types of ligands may form metal complexes with quite different properties than their less sterically encumbered counterparts.

As part of our work involving the development of model compounds for non-heme iron-oxo proteins [6], we became interested in the synthesis of mononuclear iron complexes which are capped by bulky-appended tridentate macrocycles. Recently, Wieghardt and coworkers have reported the synthesis of *N,N′,N″*-triisopropyl-1,4,7-triazacyclononane (**1**) and the characterization of several molybdenum complexes [7]. We have independently synthesized ligand **1** [8] and report here its synthesis along with that of *N,N′,N″*-triisobutyl-1,4,7-triazacyclononane (**2**). The reactivity of **1** and **2** with iron(III) is then compared to that of the well-studied macrocycles 1,4,7-triazacyclononane (**3**) and *N,N′,N″*-trimethyl-1,4,7-triazacyclononane (**4**). Interestingly, unlike **3** and **4**, under essentially identical metallation conditions neither macrocycle **1** nor **2** coordinate the iron(III) ion.

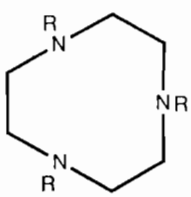

1 R = $CH(CH_3)_2$
2 R = $CH_2CH(CH_3)_2$
3 R = H
4 R = CH_3

*Author to whom correspondence should be addressed.

SSDI 0020-1693(93)03718-P

Experimental

Materials and apparatus

1,4,7-Triazacyclononane trihydrochloride was prepared according to a literature procedure [9]. 2-Bromopropane, isobutyryl chloride and $FeCl_3 \cdot 6H_2O$ were obtained from Aldrich Chemical Co. All other reagents and solvents were of reagent grade quality, purchased commercially, and used without further purification, unless otherwise noted. Proton and carbon NMR spectra were recorded on a General Electric QE-300 (300 MHz) spectrometer. Mass spectra were obtained on either a Finnigan-MAT 4023 or a Finnigan-MAT TSQ-70 instrument. Elemental analyses were performed by Atlantic Microlab.

Syntheses

Preparation of N,N',N''-trisopropyl-1,4,7-triazacyclononane (1)

This macrocycle has been independently synthesized by both Wieghardt and co-workers [7a] and our group [8]

A solution containing 1,4,7-triazacyclononane trihydrochloride (1.00 g; 4.20 mmol), 2-bromopropane (1.97 ml; 20.98 mmol) and triethylamine (3.50 ml) in acetonitrile (60 ml) was stirred and heated at reflux under a nitrogen atmosphere for 24 h. The solvent was removed on a rotary evaporator. The residue was taken up in $CHCl_3$ and washed with 1 N NaOH The organic layer was dried over $MgSO_4$. Following removal of the $MgSO_4$ by filtration and the $CHCl_3$ on a rotary evaporator, the crude product was dried *in vacuo*. There were two phases to this crude product, a dark brown semi-solid and a thin amber oil. The thin amber oil (415 mg) was separated from the semi-solid impurities with a pipet and found to be pure **1** (as judged by its ^{1}H NMR spectrum). Alternatively, pure **1** was obtained as a thin yellow oil following column chromatography on alumina (3% $CH_3OH/CHCl_3$, as eluent): yield 39%; ^{1}H NMR δ 0.93 (18H, d, CH_3), 2.60 (12H, s, NCH_2CH_2N), 2.84 (3H, septet, CH); ^{13}C NMR δ 18.29, 52.79, 54.40; EI MS *m/e* 255 (M^+); HR EI MS *m/e* 255.2657 (M^+) (calc. for $C_{15}H_{33}N_3$, *m/e* 255.2674).

Preparation of N,N'N''-trisobutyl-1,4,7-triazacyclononane (2)

(a) To a flame-dried 250 ml round-bottomed flask was added 1,4,7-triazacyclononane trihydrochloride (444 mg; 3.44 mmol), triethylamine (3 ml), and freshly distilled CH_2Cl_2 (80 ml). Isobutyryl chloride (1.15 ml; 11.00 mmol) was then added dropwise through a syringe needle while the solution was stirred at room temperature under a nitrogen atmosphere. After stirring until all of the 1,4,7-triazacyclononane was dissolved (approximately 30 min), excess isobutyryl chloride was quenched by the addition of water (10 ml). The reaction mixture was poured into a separatory funnel and the organic layer was dried over $MgSO_4$. Pure *N,N',N''*-tri(isopropylcarbonyl)-1,4,7-triazacyclononane (988 mg) was obtained as a white solid following column chromatography on silica gel (5% $CH_3OH/CHCl_3$, eluent): yield 85%; ^{1}H NMR δ 1.08 (18H, d, CH_3), 2.69 (3H, septet, CH), 3.38 (6H, t, NCH_2CH_2N), 3.69 (6H, t, NCH_2CH_2N), ^{13}C NMR δ 19.50, 30.51, 48.29, 51.33, 178.42; EI MS *m/e* 340 (MH^+).

(b) A flame-dried, 100 ml, 3-necked round-bottomed flask was charged with 1 M $LiAlH_4$ in THF (15 ml). To this was added, dropwise, a solution of *N,N',N''*-tri(isopropylcarbonyl)-1,4,7-triazacyclononane (988 mg) dissolved in dry CH_2Cl_2 (10 ml) at room temperature under a nitrogen atmosphere. After stirring the reaction overnight, $Na_2SO_4 \cdot 10H_2O$ was added to quench the excess $LiAlH_4$. The solvents were then removed on a rotary evaporator and the residue was taken up in $CHCl_3$ and washed with 1 N NaOH. The organic layer was combined and dried over $MgSO_4$. Following the removal of solvent and drying *in vacuo*, pure **2** (846 mg) was obtained quantitatively as a white solid. ^{1}H NMR δ 0.89 (18H, d, CH_3), 1.66 (3H, m, CH), 2.22 (6H, d, $NCH_2CH(CH_3)_2$), 2.73 (12H, s, NCH_2CH_2N); ^{13}C NMR δ 21.09, 26.88, 56.26, 67.85; EI MS *m/e* 297 (M^+); HR MS *m/e* 297.3146 (M^+) (calc. for $C_{18}H_{39}N_3$, *m/e* 297.3144).

Preparation of $(1 \cdot H)^+FeCl_4^-$ (5)

This salt has been independently prepared by both Wieghardt and co-workers [7a] and our group [8].

To a solution of **1** (136 mg) in 50 ml of 2-propanol (or ethanol) was added $FeCl_3 \cdot 6H_2O$ (146 mg). This caused the immediate formation of a yellow precipitate which was filtered and washed with IPA and then ethyl ether. Red crystals of **5** were grown by the evaporation of a methanol/2-propanol solution in which the yellow precipitate was dissolved. *Anal.* Calc. for $C_{15}H_{34}N_3FeCl_4$: C, 39.68; H, 7.49; N, 9.26. Found: C, 39.12; H, 7.38; N, 9.00%. This complex was characterized further by X-ray crystallography.

Preparation of $(2 \cdot H)^+FeCl_4^-$ and $(2\ H)^+_2(Fe_2OCl_6)^{2-}$ (6)

To a solution of **2** (51.3 mg) in 50 ml of 2-propanol (or ethanol) was added $FeCl_3 \cdot 6H_2O$ (47.2 mg) The yellow solution which formed was then allowed to stand for 24 h. At this time, the yellow–orange crystals of $(\mathbf{2} \cdot H)_2(Fe_2OCl_6)$ which had formed were removed by filtration. *Anal.* Calc for $C_{36}H_{80}N_6Fe_2OCl_6 \cdot 1H_2O$: C, 45.36; H, 8.68; N, 8.82. Found: C, 45.12; H, 8.41; N, 8.62%. This complex was characterized further by X-ray crystallography.

Alternatively, to a solution of **2** (40.4 mg) in 40 ml of methanol was added $FeCl_3 \cdot 6H_2O$ (37.0 mg). This resulted in the formation of a yellow solution which upon evaporation produced red crystals of $(2 \cdot H)^+ FeCl_4^-$. *Anal.* Calc. for $C_{18}H_{40}N_3FeCl_4 \cdot 1H_2O$: C, 42.18; H, 8.27; N, 8.20. Found: C, 42.76; H, 8.06; N, 8.32%.

X-ray crystallography

Crystal structures of 5 and 6

The data crystal for **5** was a red prism that was cut from a larger crystal and had approximate dimensions $0.3 \times 0.4 \times 0.6$ mm, while the data crystal for **6** was a yellow plate of approximate dimensions $0.2 \times 0.4 \times 0.5$ mm. **5** was crystallized by slow evaporation from methanol with a small amount of isopropyl alcohol while **6** was crystallized by slow evaporation of a methanol solution. Data for both crystals were collected on a Nicolet P3 diffractometer, equipped with a graphite monochromator, using Mo Kα radiation ($\lambda = 0.71073$ Å) (Table 1). The data were collected using the omega scan technique with a scan width of 1.2°. The scan rate was 5–10°/min for **5** and a constant 10°/min for **6**. For **5**, four reflections (3, 9, −3; −4, −6, −7; −5, −8,2; 4, −6, 7) were remeasured every 96 reflections to monitor instrument and crystal stability. For **6**, two reflections (−1, 1, −7; 1, −2, 5) were remeasured every 98 reflections. A smoothed curve of the intensities of these check reflections was used to scale the data. The scaling factor ranged from 0.920 to 1.00 with the intensities of the standards showing a gradual decline with time for **5** and from 0.971 to 1.000 for **6**. The data were also corrected for Lp effects and, for **6**, absorption. The absorption correction was based on measured crystal faces. No absorption correction was applied for **5** because of the highly irregular shape of the data crystal. The crystal system for **5** is orthorhombic, space group *Pbca* (No. 61) as uniquely determined from systematically absent reflections. The structure was solved by direct methods and refined by full-matrix least-squares. A difference electron density map revealed the positions of most hydrogen atoms including one near N1. However, these atoms did not refine well and were idealized (C–H, 0.96 Å) with refined isotropic thermal parameters. Because of the electron density in a geometrically reasonable position near N1, it was assumed to be the protonated nitrogen atom. The crystal system for **6** is triclinic and the space group is $P\bar{1}$ (No. 2). The structure was solved by direct methods and refined by full-matrix least-squares Most of the hydrogen atoms were located from a difference map and refined with isotropic temperature factors. The hydrogen atoms for methyl carbons, C17, C20 and C21, and methine carbon, C19, were calculated in idealized positions (C–H, 0.96 Å) with isotropic thermal parameters fixed at $1.2 \times U_{eq}$ of the relevant atom. The oxygen atom of the $(Fe_2OCl_6)^{2-}$ anion lies on an inversion center at 1, 0, $\frac{1}{2}$. The function, $\Sigma w(|F_o| - |F_c|)^2$, was minimized, where $w = 1/(\sigma(F_o))^2$ and $\sigma(F_o) = 0.5kI^{-1/2}[(\sigma(I))^{2+} (0.02I)^2]^{1/2}$. The intensity, **I**, is given by $(I_{peak} - I_{background}) \times$ (scan rate), 0.02 is a factor to downweight intense reflections and to account for instrument instability and k is the correction due to Lp effects and decay. Sigma(I) was estimated from counting statistics; $\sigma(I) = [(I_{peak} + I_{background})^{1/2} \times$ (scan rate)]. The structure solution and refinement were done using SHELXTL-PLUS [10]. The scattering factors for the non-H atoms were taken from Cromer and Mann [11], with anomalous-dispersion corrections taken from Cromer and Liberman [12], while scattering factors for the H atoms were obtained from Stewart *et al.* [13]; the linear absorption coefficient was calculated from values found in the International Tables for X-ray Crystallography [14]. Other computer programs are listed in ref. 11 of Gadol and Davis [15].

TABLE 1. Crystallographic data for $(C_{15}H_{34}N_3)FeCl_4$ (**5**) and $(C_{18}H_{40}N_3)_2Fe_2O_2Cl_6$ (**6**)

	5	**6**
Chemical formula	$C_{15}H_{34}N_3FeCl_4$	$C_{36}H_{80}N_6Fe_2O_2Cl_6$
a (Å)	14.921(2)	9.3543(10)
b (Å)	17 765(2)	10.1002(11)
c (Å)	17 414(2)	14.4167(14)
α (°)	90.0	85.185(8)
β (°)	90.0	73.395(8)
γ (°)	90 0	73.198(8)
V (Å^3)	4616.0(10)	1249 6(2)
Z	8	1
$F(000)$	1912	508
Formula weight	454 11	953.48
Space group	*Pbca*	$P\bar{1}$
T (°C)	−75	25
λ (Mo Kα) (Å)	0 7107	0.7107
ρ_{calc} (g/cc)	1.31	1.27
μ (cm^{-1})	11.23	9.399
Transmission coefficient	not applied	0 6414 - 0.8505
Total reflections	5244	5090
Reflections ($F_o > 4\sigma(F_o)$)	3061	3078
$R(F)$[a]	0.0593	0.0552
$R_w(F)$	0 0645	0.0552

[a] $R = \Sigma(|F_o| - |F_c|)/\Sigma|F_o|$, $R_w = [\Sigma w(|F_o| - |F_c|)^2/\Sigma w(|F_o|)^2]^{1/2}$.

Fractional coordinates and equivalent isotropic thermal parameters for **5** and **6** are given in Tables 2 and 3, respectively. Bond lengths and angles are given in Tables 4 and 5.

Results and discussion

Macrocycle synthesis

Using methods similar to that recently reported by Haselhorst *et al.* [7a], macrocycle **1** was produced in

TABLE 2 Fractional coordinates and equivalent isotropic thermal parameters (Å^2) for the non-hydrogen atoms of **5**

Atom	x	y	z	U
Fe1	0 15754(4)	0 68447(4)	0 80498(3)	0 0444(2)
Cl1	0 18120(10)	0 79114(7)	0 86465(7)	0 0629(5)
Cl2	0 10940(10)	0 70816(9)	0 68900(7)	0 0745(6)
Cl3	0 28261(10)	0 62153(10)	0 79836(8)	0 0824(6)
Cl4	0 05713(10)	0 62272(9)	0 86988(8)	0 0778(6)
N1	0 1397(2)	0 3156(2)	0 5638(2)	0 0374(12)
C2	0 2267(3)	0 3116(3)	0 5229(3)	0 062(2)
C3	0 2932(3)	0 3633(3)	0 5583(3)	0.061(2)
N4	0.2514(3)	0 4353(2)	0.5801(2)	0.0434(12)
C5	0.2639(3)	0 4559(4)	0.6602(3)	0.063(2)
C6	0.2154(4)	0 4079(4)	0.7154(3)	0.072(3)
N7	0.1212(2)	0 3929(2)	0.6958(2)	0.0414(13)
C8	0 984(4)	0 3145(3)	0 7007(3)	0.063(2)
C9	0.1361(4)	0 2699(3)	0 6350(3)	0 057(2)
C10	0.0567(4)	0 3062(3)	0 5148(3)	0 069(2)
C11	0 0357(4)	0 3731(3)	0 4715(4)	0 080(3)
C12	0 0625(5)	0 2339(3)	0 4674(3)	0 075(3)
C13	0 2725(4)	0 4936(4)	0.5224(4)	0 076(2)
C14	0.3675(5)	0 5252(5)	0 5288(4)	0 097(3)
C15	0 2040(5)	0 5511(4)	0.5188(6)	0.107(3)
C16	0 0602(5)	0 4456(4)	0.7344(3)	0.078(3)
C17	− 0 0193(4)	0 4642(4)	0.6879(3)	0 075(2)
C18	0 0361(5)	0 4219(4)	0.8168(3)	0 080(3)

For anisotropic atoms, the U value is U_{eq}, calculated as $U_{eq} = \frac{1}{3}\Sigma_i\Sigma_j U_{ij} a^*_i a^*_j A_{ij}$ is the dot product of the ith and jth direct space unit cell vectors

TABLE 3 Fractional coordinates and equivalent isotropic thermal parameters (Å^2) for the non-hydrogen atoms of **6**

Atom	x	y	z	U
Fe	0 93629(7)	0 10807(6)	0 59927(4)	0 0532(3)
Cl1	0 6849(2)	0 22007(13)	0 62441(10)	0 0769(6)
Cl2	0 9655(2)	− 0 0146(2)	0 73042(11)	0 0964(7)
Cl3	1 0758(2)	0 2564(2)	0 57589(12)	0 1051(8)
N1	0 5228(4)	0 2753(3)	0 3613(3)	0.047(2)
C2	0 3763(6)	0 3900(5)	0 3916(4)	0.061(2)
C3	0 2672(6)	0 3847(6)	0 3314(4)	0.061(2)
N4	0 3537(4)	0 3608(3)	0 2302(3)	0.052(2)
C5	0 3349(6)	0 2473(5)	0 1831(4)	0 060(2)
C6	0 4009(6)	0 1056(5)	0 2249(4)	0 058(2)
N7	0 5595(4)	0 0846(3)	0.2299(3)	0.0477(15)
C8	0 5904(6)	0 0291(5)	0.3211(4)	0 059(2)
C9	0 5059(7)	0 1371(5)	0 4001(4)	0 062(2)
C10	0 6629(6)	0 3040(6)	0 3749(4)	0 061(2)
C11	0 7221(6)	0 4107(5)	0 3059(4)	0 065(2)
C12	0 8591(11)	0 4345(11)	0 3345(7)	0.111(5)
C13	0 7745(8)	0 3640(7)	0 2020(4)	0.069(3)
C14	0.3709(6)	0 4856(5)	0 1718(4)	0.065(2)
C15	0.2308(7)	0 5833(5)	0 1474(4)	0 079(3)
C16	0.1672(10)	0.5229(9)	0 0800(6)	0 108(4)
C17	0.2738(8)	0.7123(6)	0 1009(5)	0 118(4)
C18	0 6819(6)	0 0368(5)	0 1411(4)	0 055(2)
C19	0.7067(7)	− 0.1033(5)	0 1014(4)	0.085(3)
C20	0.7129(12)	− 0 2168(6)	0 1618(6)	0.209(6)
C21	0.8380(8)	− 0 1241(6)	0 0066(4)	0.102(3)
O1	1 0	0 0	0 5	0.139(4)

For anisotropic atoms, the U value is U_{eq}, calculated as $U_{eq} = \frac{1}{3}\Sigma_i\Sigma_j U_{ij} a^*_i a^*_j A_{ij}$ where A_{ij} is the dot product of the ith and jth direct space unit cell vectors.

40% yield by the reaction of TACN with 2-bromopropane [8]. Interestingly, unlike TACN, **1** is a relatively thin oil. In fact, following the removal of the solvent from the reaction mixture, **1** can be isolated in quite pure form using only a pipet. This physical characteristic is considered reflective of the significant steric hindrance about the nitrogen atoms of the macrocycle provided by the isopropyl groups (i.e. relative to the parent compound, TACN, intermolecular forces are significantly reduced in **1**).

The first step to synthesizing **2** is the reaction of isobutyryl chloride with TACN (Scheme 1). Reduction of the resulting triamide is then achieved in quantitative yield using 1.0 M $LiAlH_4$ in THF. This two-step reaction sequence produces **2** as a waxy, white solid in over 80% yield.

Reactions of Fe(III) with 1 and 2

The reaction of **1** with $FeCl_3 \cdot 6H_2O$ in isopropyl alcohol (IPA) produces a yellow precipitate, **5**, which was originally thought to be a 1:1 metal complex. Both **3** and **4** have been shown to react with ferric chloride to form yellow 1:1 iron complexes that are relatively insoluble in alcoholic solvents [3, 16]. Unlike the iron(III) complexes of **3** and **4**, however, **5** has appreciable solubility in ethanol and is very soluble in methanol.

Slow evaporation of a methanolic solution of **5** in the presence of isopropanol produced red, X-ray quality crystals. As shown in Fig. 1, the X-ray structure determination reveals that macrocycle **1** is not coordinated to the iron(III) ion. Instead, **1** is protonated and a tetrahedral $FeCl_4^-$ anion serves as the counterion. The proton is localized on N1, but shared with the other two nitrogen atoms, N4 and N7, through hydrogen bonds. This results in the lengthening of the C–N bonds to N1 (N1–C2 = 1.482(6); N1–C9 = 1.483(6) Å) relative to the other C–N bonds in the macrocycle (N4–C3 = 1.472(7); N4–C5 = 1.454(6); N7–C6 = 1.471(7); N7–C8 = 1.436(6) Å).

Attempts to deprotonate the TACN macrocycle in **5** with triethylamine resulted in the formation of insoluble, rust-colored iron oxide oligomers formed by the basic hydrolysis of iron(III) chloride and not in a complex involving ligand **1**.

The reaction of **2** with $FeCl_3 \cdot 6H_2O$ in 2-propanol produced a yellow–orange solution which upon standing (24 h), gives yellow–orange crystals of $(\mathbf{2} \cdot H)_2(Fe_2OCl_6)$ (**6**). The solubility of **6** in ethanol and methanol mirrors that of **5**. An X-ray structure determination reveals that, as in **5**, the TACN macrocycle in **6** is protonated

TABLE 4. Bond lengths (Å) and angles (°) for non-hydrogen atoms of the macrocycle in **5**

1	2	3	1–2	1–2–3
C2	N1	C9	1.482(6)	114 0(4)
C9	N1	C10	1.483(6)	112 4(4)
C10	N1	C2	1.513(7)	116 1(4)
C3	C2	N1	1.486(7)	110 8(4)
N4	C3	C2	1.472(7)	111 2(4)
C5	N4	C13	1.454(6)	116 7(4)
C5	N4	C3		114 3(4)
C13	N4	C3	1.477(7)	110 1(4)
C6	C5	N4	1 473(8)	114 7(5)
N7	C6	C5	1 471(7)	115.0(4)
C8	N7	C16	1 436(6)	116 4(4)
C8	N7	C6		112 9(4)
C16	N7	C6	1 470(8)	111 6(4)
C9	C8	N7	1.502(7)	112 2(4)
N1	C9	C8		111 2(4)
C11	C10	C12	1.442(8)	115 0(5)
C11	C10	N1		112.5(5)
C12	C10	N1	1.529(8)	110 5(5)
C14	C13	C15	1.529(9)	113 5(6)
C14	C13	N4		113 9(5)
C15	C13	N4	1.445(10)	112 0(5)
C17	C16	C18	1.474(9)	112 7(6)
C17	C16	N7		112 9(4)
C18	C16	N7	1.538(8)	113 4(5)

to form a monocation (Fig. 2) and does not coordinate to the iron(III) cation at all. The proton is localized on N1 (N1–H = 0.81(4) Å), but is hydrogen-bonded to both N4 and N7. This results, as in **5**, in the lengthening of the C–N bonds to N1 (N1–C2 = 1.496(5); N1–C9 = 1.494(6) Å) relative to the other C–N bonds in the macrocycle (N4–C3 = 1.454(6); N4–C5 = 1.456(7); N7–C6 = 1.460(7); N7–C8 = 1.457(6) Å).

The counterion in **6** is the well-known, oxo-bridged iron dimer $Fe_2OCl_6^{2-}$ [17]. Its formation is simply a result of the hydrolysis of ferric chloride. As evidence for this, we note that two differently-colored crystals, red and yellow–orange, were isolated from these reaction mixtures depending on the conditions employed. The red crystals analyzed correctly for the presence of $FeCl_4^-$, while the yellow–orange crystals analyzed for $Fe_2OCl_6^{2-}$. In both cases, the cation is the monoprotonated form of macrocycle **2**. Relatively long reaction (or crystallization) times (24 h) result in the formation of the hydrolyzed $Fe_2OCl_6^{2-}$ anion, whereas, short reaction times (e.g. 30–60 min) result in material which contains the $FeCl_4^-$ anion.

It should be noted that the X-ray structure of the monoprotonated form of macrocycle **4**, *N*,*N*′,*N*″-trimethyl-1,4,7-triazacyclononane (**7**), has been reported by Wieghardt *et al.* [18]. It was made by the direct addition of $HClO_4$ to **4**. As in **5** and **6**, the proton in **7** is localized on one nitrogen atom while being hydrogen-bonded to the other two nitrogen atoms.

TABLE 5. Bond lengths (Å) and angles (°) for the non-hydrogen atoms of **6**

1	2	3	1–2	1–2–3
Cl1	Fe	Cl2	2 2327(14)	108 03(5)
Cl1	Fe	Cl3		110.38(6)
Cl2	Fe	Cl3	2.212(2)	108.35(7)
Cl2	Fe	O1		109.93(5)
Cl3	Fe	O1	2 203(2)	109.44(5)
O1	Fe	Cl1	1 7302(6)	110.67(5)
Fe	O1	Fe′		180(0)
C2	N1	C9	1 496(5)	113.5(4)
C9	N1	C10	1 494(6)	112 5(4)
C10	N1	C2	1.488(8)	114.8(4)
C3	C2	N1	1 530(9)	109.5(4)
N4	C3	C2	1 454(6)	110.0(4)
C5	N4	C14	1 456(7)	117.6(4)
C5	N4	C3		116.4(4)
C14	N4	C3	1.478(6)	115.9(4)
C6	C5	N4	1 532(7)	112.8(5)
N7	C6	C5	1 460(7)	112.6(4)
C8	N7	C18	1.457(7)	117.3(3)
C8	N7	C6		115.7(4)
C18	N7	C6	1.460(5)	115.9(4)
C9	C8	N7	1 520(7)	109.6(4)
N1	C9	C8		109.3(4)
C11	C10	N1	1.520(8)	114 9(5)
C12	C11	C13	1 538(13)	109.7(5)
C12	C11	C10		107.8(6)
C13	C11	C10	1.508(8)	112.0(5)
C15	C14	N4	1.507(8)	119.3(5)
C16	C15	C17	1.519(13)	108.9(6)
C16	C15	C14		114.3(5)
C17	C15	C14	1.520(8)	108 6(5)
C19	C18	N7	1.502(7)	119.6(4)
C20	C19	C21	1.378(8)	114 8(5)
C20	C19	C18		120.0(6)
C21	C19	C18	1.536(7)	108 4(5)

Fe′ is related to Fe by $2-x$, $-y$, $1-z$.

The only structural difference between the protonated macrocycle in **7** and those in **5** and **6** is the ring conformation. The minimum energy forms of nine-membered rings and their modes of interconversion have been investigated by Hendrickson [19] and, subsequently, by Dale [20], and Evans and Boeyens [21]. Of the sixteen symmetrical conformations, the lowest energy form, by 2.2 kcal/mol, has D_3 symmetry and is known as a twist-boat-chair (TBC). A comparison of the torsion angles of the 16 classical forms to actual X-ray structural data reveals the conformations of the TACN rings in **5**, **6** and **7**. As shown in Table 6, the torsion angles of the TACN macrocycles in **5** and **6** are very similar to the idealized angles calculated for the TBC form. The TACN ring in **7**, however, more closely resembles the higher energy boat-chair (BC) form (C_{3v} symmetry). In the case of **7**, the hydrogen bonding interactions between N4, N7 and the proton on N1 apparently stabilize the higher energy boat-chair

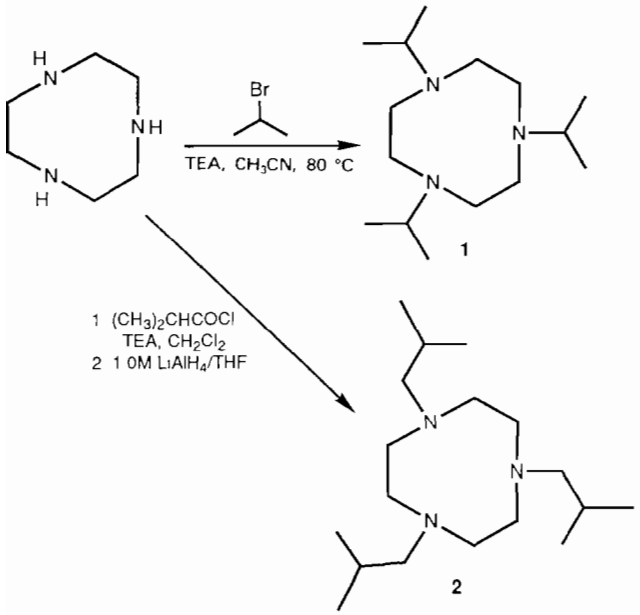

Scheme 1

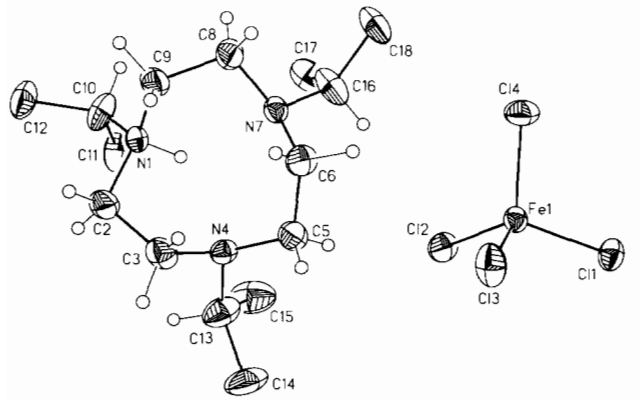

Fig 1 View of $(1\ H)^+(FeCl_4)^-$ (**5**) showing the atom labelling scheme Thermal ellipsoids are scaled to the 30% probability level. H atoms are of an arbitrary size, with some omitted for clarity.

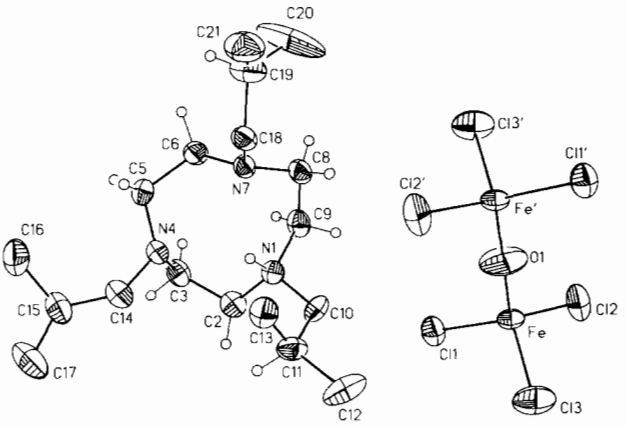

Fig 2 View of $(2\ H)^+_2(Fe_2OCl_6)^{2-}$ (**6**) with one of the macrocyclic cations omitted for clarity The oxygen atom of the Fe dimer lies on an inversion center at 1, 0, ½ Atoms marked by ′ are related by $2-x$, $-y$, $1-z$ Thermal ellipsoids are scaled to the 30% probability level H atoms are of an arbitrary size, with some omitted for clarity

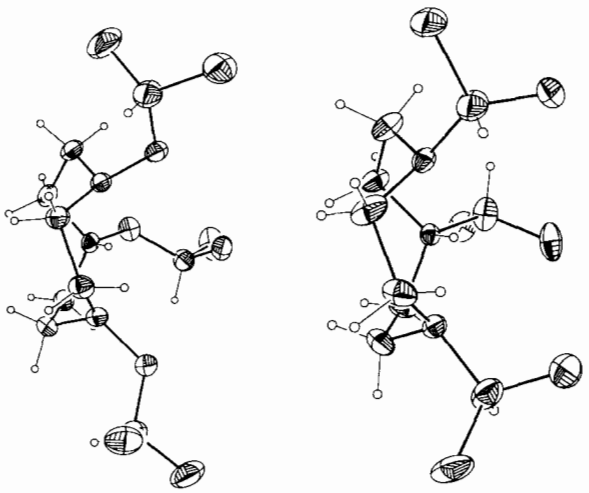

Fig 3 Side-on views of **5** and **6** showing the pocket that is formed by the three bulky pendant alkyl groups.

conformation. In **5** and **6**, however, we propose that this stabilization is countered by the steric interactions of the bulky isopropyl and isobutyl groups, respectively. This constraint is relieved by the twisting of the macrocycle into the TBC conformation.

Conclusions

We have synthesized the two macrocycles *N,N′,N″*-triisopropyl-1,4,7-triazacyclononane (**1**) and *N,N′,N″*-triisobutyl-1,4,7-triazacyclononane (**2**). Under the same metallation conditions used in the synthesis of **5** and **6**, both **3** and **4** coordinate as tridentate ligands to the iron(III) ion. Though the protonation constants have yet to be rigorously determined for **1** or **2**, they are expected to be quite similar to those reported for **4** [22] since the macrocyclic amines in all three cases are tertiary. It would appear then that the reduced affinity of **1** and **2** for the iron(III) ion is based primarily on the steric effects of the bulky isopropyl and isobutyl appendages, respectively. In Fig. 3, side-on views of the protonated macrocycles in **5** and **6** show the isopropyl and isobutyl groups to be all directed toward the same side of the macrocycle. In each case, the lone pairs associated with N4 and N7 and the proton on N1 are directed toward the center of the macrocycle. The bulky alkyl groups create a congested cavity in each macrocycle into which metal ions must travel to coordinate to the nitrogen lone pairs. However, recent work by Wieghardt and co-workers demonstrates the use of aprotic solvents and elevated temperatures to facilitate the coordination of ligand **1** to molybdenum [7]. Similar reaction con-

TABLE 6. Torsion angles (°), ω, calculated for the two classical forms [21] TBC and BC and measured by X-ray diffraction for **5**, **6** and **7**

	ω_1	ω_2	ω_3	ω_4	ω_5	ω_6	ω_7	ω_8	ω_9
TBC	−57	130	−57	−57	130	−57	−57	130	−57
BC	−114	0	114	−114	0	114	−114	0	114
5	−46	131	−74	−33	132	−81	−40	125	−69
6	−50	133	−69	−42	138	−77	−44	128	−66
7	−113	7	91	−103	11	91	−108	18	95

ditions have yet to be explored for the coordination of iron(III).

Supplementary material

Full details of the X-ray structure of complexes **5** and **6**, including atomic coordinates, bond lengths and angles, and thermal parameters have been deposited at the Cambridge Crystallographic Data Center.

Acknowledgements

J.L.S. thanks the NIH (Grant No. GM 36348), the NSF (PYI Award 1986), and the Dreyfus Foundation (New Faculty Award, 1984; Teacher-Scholar Award 1988) for financial support for this work.

References

1 (a) G A. Melson, *Coordination Chemistry of Macrocyclic Compounds*, Plenum, New York, 1979, (b) L F Lindoy, *The Chemistry of Macrocyclic Ligand Complexes*, Cambridge University Press, Cambridge, UK, 1989.
2 P Chaudhuri and K. Wieghardt, *Prog Inorg Chem., 35* (1987) 329–436
3 (a) K. Wieghardt, K. Pohl and W Gebert, *Angew Chem*, *95* (1983) 739–740, (b) J.R. Hartman, R.L Rardin, P. Chaudhuri, K. Pohl, K Wieghardt, B Nuber, J Weiss, G C. Papaefthymiou, R.B. Frankel and S.J. Lippard, *J Am Chem Soc*, *109* (1987) 7387–7396
4 P V Bernhardt and G.A. Lawrance, *Coord Chem Rev*, *104* (1990) 297–343.
5 T Beissel, B S P C. Della Vedova, K Wieghardt and R Boese, *Inorg Chem*, *29* (1990) 1736–1741.
6 (a) J L. Sessler, J W Sibert and V Lynch, *Inorg Chem*, *29* (1990) 4143–4146, (b) J.L Sessler, J.D Hugdahl, V. Lynch and B. Davis, *Inorg Chem*, *30* (1991) 334–336, (c) J.L Sessler, J W Sibert, V Lynch, J T Markert and C L Wooten, *Inorg Chem*, *32* (1993) 621–626
7 (a) G. Haselhorst, S. Stoetzel, A Strassburger, W. Walz, K Wieghardt and B Nuber, *J Chem Soc, Dalton Trans.*, (1993) 83–90, (b) S Stoetzel, K. Wieghardt and B. Nuber, *Inorg Chem*, *32* (1993) 2128–2131
8 J.W. Sibert, *Ph D Dissertation*, University of Texas at Austin, TX, 1991.
9 (a) T.J Atkins, J.E Richman and W F Oettle, *Org Synth*, *58* (1978) 86–98, (b) K. Wieghardt, W Schmidt, B Nuber and J. Weiss, *Chem. Ber*, *112* (1979) 2220–2230.
10 G.M. Sheldrick, *SHELXTL-PLUS*, Siemens Analytical X-ray Instruments, Inc Madison, WI, 1991
11 D.T. Cromer and J.B. Mann, *Acta Crystallogr, Sect A, 24* (1968) 321–324
12 D T Cromer and D Liberman, *J Chem Phys*, *53* (1970) 1891–1898
13 R F. Stewart, E R Davidson and W T Simpson, *J Chem Phys*, *42* (1965) 3175–3187.
14 *International Tables for X-ray Crystallography*, Vol IV, Kynoch, Birmingham, UK, 1974, p 55
15 S M. Gadol and R.E Davis, *Organometallics, 1* (1982) 1607–1613
16 K. Wieghardt, K Pohl and D Ventur, *Angew Chem, Int Ed Engl*, *24* (1985) 392–393.
17 G Haselhorst, K Wieghardt, S Keller and B Schrader, *Inorg. Chem*, *32* (1993) 520–525, and refs therein
18 K. Wieghardt, S Brodka, K. Peters, E.M Peters and A Simon, *Z Naturforsch, Teil B, 42* (1987) 279–281
19 (a) J B. Hendrickson, *J Am Chem Soc*, *86* (1964) 4854–4866, (b) *89* (1967) 7047–7061
20 (a) J. Dale, *Acta Chem Scand*, *27* (1973) 1115–1129; (b) 1130–1148
21 D G Evans and J.C A Boeyens, *Acta Crystallogr, Sect B, 46* (1990) 524–532, and refs therein
22 G C Geraldes, M.C. Alpoim, M P.M. Marques, A.D. Sherry and M Singh, *Inorg Chem*, *24* (1985) 3876–3881.